scientific reports

OPEN

Characterisation of AZ31/TiC composites fabricated via ultrasonic vibration assisted friction stir processing

T. Satish Kumar[1]✉, Titus Thankachan[2], Robert Čep[3] & Kanak Kalita[4,5]✉

In this study, the effect of ultrasonic vibration during Friction Stir Vibration Processing (FSVP) on the microstructure and mechanical behaviour of AZ31/TiC surface composites was investigated. Specifically, Titanium Carbide (TiC) particles were introduced as a reinforcement (15 vol%) into the magnesium alloy AZ31 using both Friction Stir Processing (FSP) and FSVP. Comprehensive examinations were carried out to analyse the microstructure, hardness, and tensile behaviour of the resulting composites. The study revealed significant improvements in mechanical properties due to the application of ultrasonic vibration during FSP. Firstly, the stir zone region was found to be free from voids, enhancing material flow and promoting even dispersion of TiC powders within the matrix. Secondly, refinement of grains was observed due to dynamic recrystallization and the pinning effect imposed by TiC particles, leading to the formation of more dislocations in the composite and indicating a considerable alteration in the material's structure. Importantly, the vibration during FSP introduced an auxiliary energy source, resulting in a remarkable enhancement in both hardness and tensile strength. Compared to the AZ31/15 vol% TiC FSP composite, the composites produced via FSVP exhibited a grain size reduction of about 64% and improvements in hardness and ultimate tensile strength (UTS) of about 55% and 21%, respectively. Notably, these improvements were achieved without compromising the ductility of the composite, which remained at appreciable levels.

Keywords AZ31, magnesium, FSP, FSVP, ultrasonic vibration, Mechanical properties

Improving material flow through the application of ultrasonic and vibration techniques represents an innovative approach for enhancing both the mechanical properties and microstructural refinement in alloys and composites when subjected to Friction Stir Processing (FSP)[1–3]. The surface modification technology known as FSP is derived from Friction Stir Welding (FSW) and is extensively employed to fabricate surface composites[4]. Balakrishnan et al.[5] fabricated AZ31/TiC magnesium matrix composites via friction stir reaction. They indicated that TiC particles were evenly dispersed throughout the magnesium matrix without the emergence of clusters, and there was no chemical reaction occurring at the interface between the magnesium matrix and the TiC particles. Navazani et al.[6] used FSP to develop magnesium-based composites reinforced with 5 μm titanium carbide particles on the surface of an AZ31 magnesium alloy sheet. The findings indicated that the mean grain size of the developed Mg/TiC surface composites significantly reduced, and the average hardness of the stirred zone increased from 50 Vickers to 79 Vickers.

Researchers have explored hybrid techniques that combine traditional FSP with an ultrasonic source to enhance the characteristics of the developed surface composites[1]. In addition to the enhancement of material flow, researchers have identified several other properties improved by vibration, as outlined by Tian et al.[7], including alterations in the static and dynamic volume within the nugget zone. Along with this, refinement in grain structure was also observed due to increased dislocation density. Extensive research efforts have been devoted to investigating the role of vibration during friction stir welding and processing on both welded joints

[1]Department of Mechanical Engineering, Amrita School of Engineering, Amrita Vishwa Vidyapeetham, Coimbatore 641112, India. [2]Department of Mechanical Engineering, Karpagam College of Engineering, Coimbatore, India. [3]Department of Machining, Assembly and Engineering Metrology, Faculty of Mechanical Engineering, VSB-Technical University of Ostrava, Ostrava 70800, Czech Republic. [4]Department of Mechanical Engineering, Vel Tech Rangarajan Dr. Sagunthala R&D Institute of Science and Technology, Avadi 600 062, India. [5]Jadara University Research Center, Jadara University, Irbid, Jordan. ✉email: t_satishkumar@cb.amrita.edu; drkanakkalita@veltech.edu.in; kanakkalita02@gmail.com

and processed materials, as evidenced in studies[8–10]. The consensus in the field generally recognizes that the incorporation of vibration in processes like FSW and FSP leads to notable enhancements in fluidity, effective material mixing, and overall material flow within the weld or stir nugget. This improvement can be attributed to the softening effect induced by ultrasonic vibration[11,12]. Notably, the application of vibration has demonstrated the capability to eliminate brittle intermetallic compounds while joining aluminium and magnesium via FSW, consequently leading to improved mechanical strength. This approach has also proved effective in the complete removal of intermetallic compounds, leading to enhanced dispersion of phases within the magnesium matrix[13].

Swathi et al.[14] carried out a study on AA7075-T651/nano-sized B_4C surface composites, exploring variations in processing parameters and particle addition. Both FSP and Ultrasonic Vibration Assisted FSP (UAFSP) were used and the Jaya algorithm was employed to optimize process parameters. Microstructure analysis of processed specimens revealed that a combination of the Zener pinning effect and dynamic recrystallization during UAFSP had a significant impact on grain refinement and the incorporation of nano B_4C particles into the surface composite. This resulted in a finer grain structure, attributed to increased strain rate and deformation. UAFSP on AA7075 alloy led to even better dispersion of nano-sized boron carbide particles into the aluminium alloy, breaking up agglomerated particles and thereby enhancing its properties. Considering the attained results, tensile strength increased to 296.11 MPa for friction stir processed samples and to 315.82 MPa for ultrasonic vibration assisted friction stir processed samples, compared to 185.88 MPa for the base metal. Furthermore, an increase in impact strength, ductility, and microhardness was observed for specimens prepared via UAFSP compared to those prepared via FSP.

Liang et al.[15] reported a hybrid approach that integrated ultrasonic-assisted extrusion with FSP to produce a composite of carbon nanotubes (CNTs) and magnesium (Mg). Their findings revealed that the ultrasonic source effectively dispersed CNT clusters, allowing them to integrate seamlessly within the magnesium alloy matrix without forming agglomerates. This integration led to significant improvements in strength and ductility. In a similar vein, Bagheri et al.[16] investigated the impact of vibration during the FSP process, specifically focusing on the AZ91/SiC composite. Their study revealed a reduction in porosity and an increase in compressive strength when vibration was applied. It was observed that vibration frequency plays a major role in dispersing reinforcement particles homogeneously into the matrix metal. In another study, Gao et al.[17] reported the use of ultrasonic vibration in the process of joining AA2024-T4 aluminium plates. An improvement in the refinement of the stir zone (SZ) and even dispersion of precipitates due to ultrasonic vibration during synthesis was observed. Consequently, this microstructural refinement contributed to the improvement of mechanical properties in the joined materials. Recently, Zhang et al.[1] studied the effect of the vibration process along with FSP on AZ31 magnesium alloy infused with CeO_2 and ZrO_2 reinforcing particles. The utilization of vibration led to several notable improvements, including the enlargement of the SZ and the effective dispersion of the reinforcing particles. This enhancement in material flow and fluidity can be attributed to the assistance provided by vibration. The research findings demonstrated that FSVP leads to a higher level of refinement with reinforcement being distributed homogeneously in the stir zone. An increase in shear strength of about 29% was observed for specimens fabricated via FSVP when compared with friction stir processed specimens.

This study delves into the influence of vibration during FSP on the properties of AZ31/TiC composites. Titanium Carbide (TiC) particles were selected as reinforcement due to their high hardness and excellent resistance to wear, electrochemical degradation, and thermal factors. The synergistic qualities of TiC when combined with magnesium alloys hold the potential to expand the applications of AZ31 magnesium alloy beyond its current uses, encompassing industries such as automotive, aviation, and aerospace. Consequently, this study aimed to investigate the microstructure and mechanical characteristics of the developed AZ31/TiC composites. The findings were then compared with samples produced via conventional FSP for comprehensive evaluation.

Experimental procedure

In this study, AZ31 magnesium alloy plates with a thickness of 8 mm were used as the base material and reinforced with 15 vol% TiC particulates. The average size of the TiC particles was approximately 5 to 10 µm. Before the synthesis of the composites, several preparatory steps were undertaken to incorporate 15 vol% TiC into the AZ31 plates. These steps included groove cutting, filling the grooves with the TiC reinforcements, and closing the grooves using a pinless tool to encapsulate the powder. Subsequently, both FSP and FSVP of the prepared specimens were carried out using an H13 steel tool with a tool tilt angle of 2°. It is noteworthy that the parameters for FSP and FSVP remained constant, with a traverse speed of 100 mm/min and a rotational speed of 900 rpm. To introduce ultrasonic vibrations, a magneto strictive transducer with an SS304 horn (RELTEC, Russia) was employed. The FSP fixture was attached to the ultrasonic vibration waveguide. This setup is schematically illustrated in Fig. 1.

During FSP, specimens were subjected to ultrasonic vibration at a constant frequency of 35 Hz and a vibration amplitude of 0.5 mm. Following the processing, the AZ31/TiC composites were cut to obtain samples for microstructural analysis, which were further prepared through grinding, polishing, and etching with a solution comprising 4 ml picric acid, 10 ml acetic acid, and 70 ml ethanol. For macro- and microstructural analysis, various microscopy and testing techniques were employed. These included a Field Emission Scanning Electron Microscope (FE-SEM), model Gemini 300 SEM. For assessing the powders, an optical microscope (OM), model MA-100 from Nikon, and a transmission electron microscope (TEM), model JEOL JEM 2100, were used for studying induced dislocations. XRD studies were conducted with an X-ray diffractometer (Shimadzu XRD-6000) using Cu Kα radiation. Electron Backscatter Diffraction (EBSD) was performed using a Field Emission Gun Scanning Electron Microscope (FEG SEM), FEI Quanta. Micro Vickers hardness testing (Mitutoyo) was carried out on the prepared composites under constant parameters, employing a 100 g load and a 10 s holding time. Tensile evaluation of the specimens was carried out using an Instron tensile testing machine as per ASTM

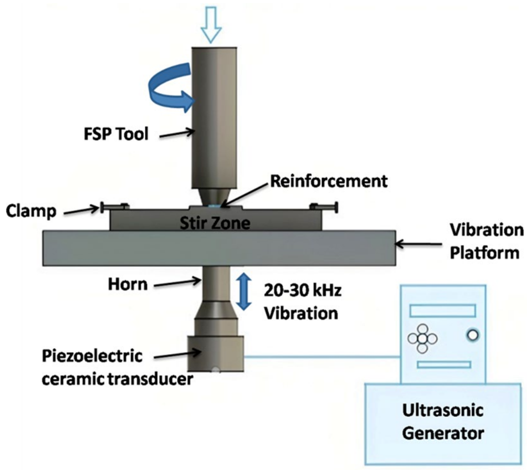

Fig. 1. Schematic view of FSP/FSVP process.

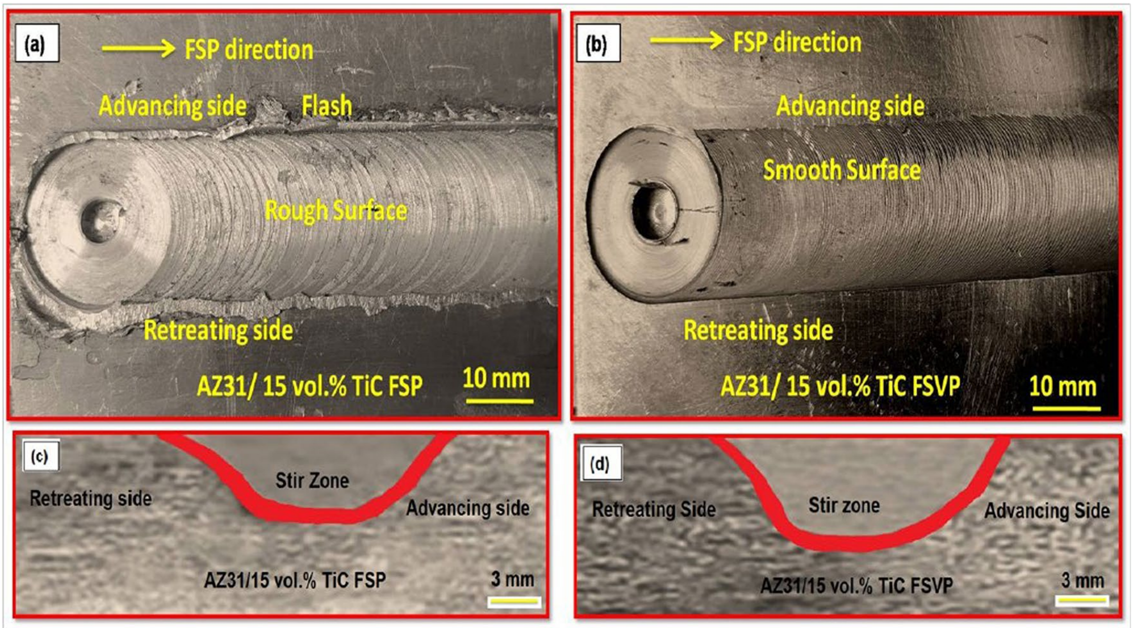

Fig. 2. Macro view of AZ31 alloy/15 vol. %TiC composites produced via (**a**) FSP and (**b**) FSVP; cross-sectional images of the composites produced via (**c**) FSP and (**d**) FSVP.

E8/E8M–08 standards, and the mechanisms behind the failure were analysed using FE-SEM micrographs of the fractured surfaces.

Results and discussion

The top surfaces of the AZ31/15 vol% TiC composites produced using FSP and FSVP techniques are shown in Fig. 2a and b, respectively. The FSP composite sample surface displays a rough texture with the presence of flash in a few places. Conversely, Fig. 2b (FSVP) reveals a smoother surface with no flash. This suggests that the improved material movement, possibly due to enhanced straining of materials through vibration, eliminated the formation of these voids. The enhanced material flow observed here is due to the reduction in flow stress, which facilitates better dispersion of TiC particles, in line with observations from similar studies[18]. Cross-sectional macro-views of the processed regions of the composites produced via FSP and FSVP are shown in Fig. 2c and d, respectively. The FSVP stir zone has greater tool penetration depth and a smoother appearance compared to the FSP stir zone.

Figure 3 displays the X-ray diffraction (XRD) patterns for the AZ31/TiC surface composites produced through both FSP and FSVP methods. The peaks corresponding to the magnesium matrix, Mg17Al12, and the reinforcing material TiC are clearly observed in Fig. 3. Notably, there are no significant traces of other

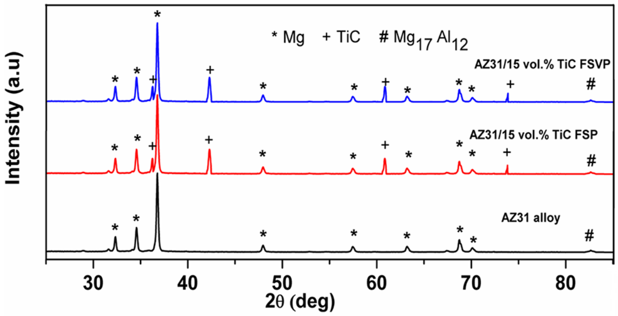

Fig. 3. XRD outline of AZ31/TiC surface composites.

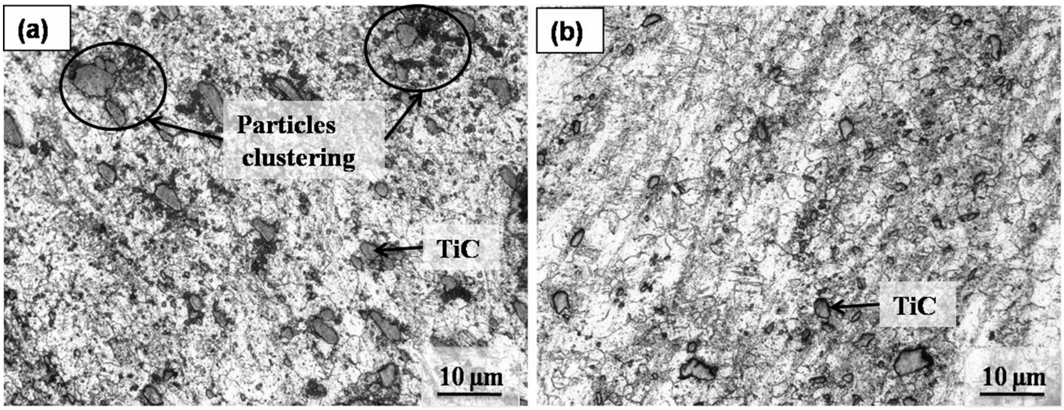

Fig. 4. Optical micrographs of AZ31/ 15 vol. %TiC composites fabricated via (**a**) FSP and (**b**) FSVP.

detrimental phases detected in any of the composite samples. It is well known that magnesium and TiC are immiscible, meaning they do not readily dissolve into each other, regardless of temperature. Studies have proven that the formation of metastable phases occurs with severe plastic deformation, and this can be monitored based on the peak broadening of magnesium in XRD patterns[19]. In the case of Fig. 3, there is no broadening of Mg peaks, confirming the absence of metastable phase formation. This absence could be attributed to the relatively brief exposure to severe deformation during the manufacturing process. It is essential to note that the matrix used in this study is not pure magnesium; it is the Mg alloy AZ31, which includes elements such as aluminium (Al). Aluminium and TiC have a strong chemical affinity and tend to form undesirable compounds like Ti_3Al at elevated temperatures and extended straining periods[20,21].

Figure 4 presents optical micrographs depicting AZ31/15 vol% TiC composites, taken at random regions within the SZ. Uniform distribution of TiC particles is observed regardless of the specific location of the micrographs. Composites produced with conventional FSP showed voids and agglomeration in a few places. Voids are open areas or cavities that exist within a solid material. Whether microscopic or macroscopic, these voids can have a substantial impact on the mechanical characteristics of the material, including its strength, density, and wear resistance. In traditional FSP, the material may exhibit poor flowability, resulting in the creation of voids. A lack of sufficient material flow around the tool can lead to the formation of empty spaces, particularly if the material fails to completely consolidate behind the tool. Voids are often formed due to particle clustering in the conventional FSP process.

In contrast, the samples produced through FSVP demonstrated uniform dispersion of TiC particulates within the SZ, as depicted in Fig. 4b. Notably, there is no area within the samples produced using FSVP where the distribution is absent. A continuous interface surrounds the particles without any interruptions, and no foreign particles are detected at this interface. The AZ31 alloy is seamlessly reinforced with the particles on all sides, with no visible pores.

SEM micrographs of the AZ31/15 vol% TiC composites in the SZ, produced via FSP and FSVP, are shown in Fig. 5a and b, respectively. The densely packed TiC particles are dispersed throughout all regions of the SZ. The spacing between these particles, known as the inter-particle distance, is consistently minimal, indicating uniform distribution of particles. A well-defined interface, as observed in Fig. 5a and b, indicates that the plasticized material fully envelops the particles' surfaces. Importantly, the TiC particles do not exhibit sharp corners, which could disrupt the even flow of the material and generate pores[22]. Figure 5b (FSVP) exhibits proper dispersion of TiC particles within the SZ, with no noticeable clustering. In contrast, Fig. 5a (without vibration) shows particle clustering in the matrix composite due to insufficient material flow. The enhanced material flow observed here can be attributed to a reduction in flow stress during FSVP, which promotes a better

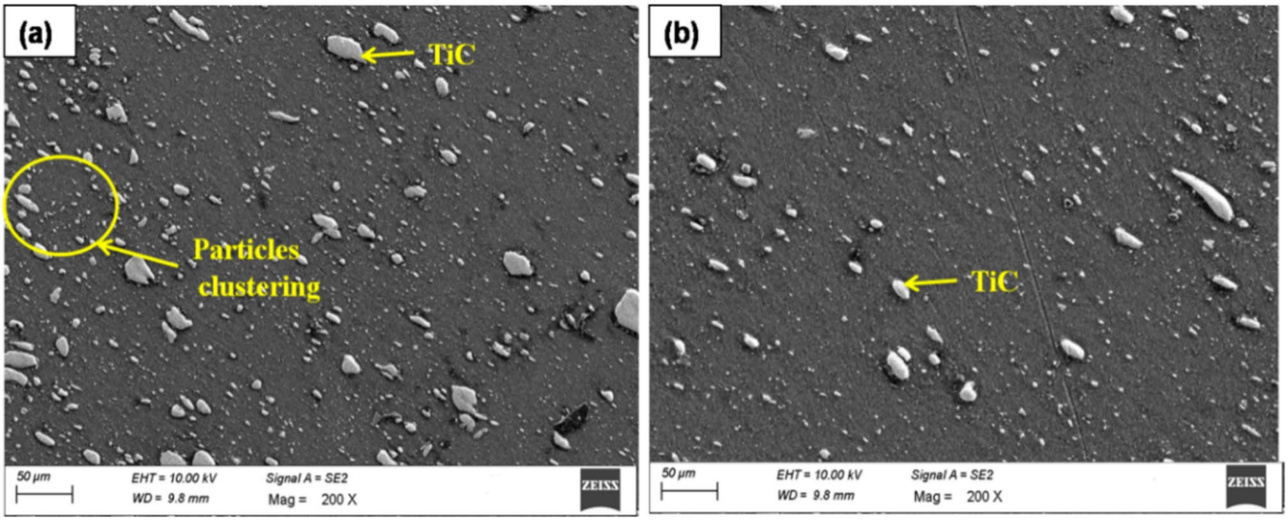

Fig. 5. SEM micrographs of AZ31/ 15 vol. %TiC composites (**a**) FSP and (**b**) FSVP.

dispersion of the reinforcement particles in the matrix, in line with previous studies[18]. This is confirmed through EDS mapping and XRD analysis. Figure 5b (FSVP) also exhibits a higher level of particle refinement compared to Fig. 5a (FSP).

An absence of significant change in the elemental spectrum at the interface suggests that no chemical reactions occurred between the alloying elements, and hence no compound formation happened. Interface characteristics play a crucial role in defining the load-bearing capability of metal matrix composites. The presence of voids and additional compounds within the interface can have adverse effects on mechanical performance. Therefore, a robust interface is more crucial than uniform distribution in enhancing the composite's mechanical properties. Similar to various studies[22–26] where deviations in the shape and size of reinforcement particles were observed after processing, this study also reports a significant reduction in particle size after FSVP, as shown in Fig. 5a and b.

Uniform dispersion of TiC particles in the AZ31 matrix metal is evident from the micrographs after FSVP, confirming the even distribution of TiC particles in the composite. To confirm the absence of diffusion or the presence of other compounds, point EDS analysis was performed on the TiC particles, as depicted in Fig. 6. The elemental spectra revealed the presence of Mg, Al, Ti, and C.

The distribution of elements in the AZ31/15 vol% TiC FSVP surface composites is shown in Fig. 7. Line scan elemental mapping of a TiC particle near the interface revealed a dramatic drop in Ti and C concentrations, indicating the absence of reactions at the interface and confirming a strong bond to the matrix. Figure 8a and b presents the Electron Backscatter Diffraction (EBSD) inverse pole figure (IPF) maps with grain boundaries of AZ31/15 vol% TiC composites fabricated using FSP and FSVP respectively. Similarly, the grain size distributions of the FSP sample and the FSVP sample is shown in Fig. 8c and d respectively. Additionally the misorientation angle distributions for the FSP sample and the FSVP sample is shown in Fig. 8e and f respectively. The AZ31 alloy consists of coarse grains with an average size of 60 µm, as explained in our previous study[27]. There is a significant reduction in grain size, with the AZ31/15 vol% TiC FSP metal matrix composite (MMC) recording an average grain size of 28 µm, as shown in Fig. 8c. With FSVP, the grain size further reduced to 8–10 µm in the AZ31/15 vol% TiC FSVP MMC, as shown in Fig. 8d. Examination of the corresponding misorientation maps in Fig. 8e and f indicates a higher percentage (40–50%) of high-angle grain boundaries in the FSVP sample compared to the FSP sample.

TEM micrographs offering insights into the microstructural characteristics of AZ31/15 vol% TiC FSVP composites are shown in Fig. 9. Figure 9a and b demonstrate a strong bond and good interfacial integrity between the matrix alloy AZ31 and the reinforcing TiC particles.

Figure 9c reveals fine grains and an even distribution of particles within the composite. Figure 9d shows the presence of a significant number of dislocations. The presence of dislocations indicates that the material has undergone plastic deformation, which can contribute to changes in mechanical properties and grain refinement[28]. The TEM micrographs in Fig. 9 display a well-dispersed reinforcement phase, excellent interfacial bonding, and the presence of dislocations within the matrix alloy AZ31. These characteristics are essential for understanding the structural properties and potential mechanical behaviour of the composites[25].

Although the TiC particles in the composite are small, they are effectively distributed throughout as depicted in Fig. 9b. Most of these particles are found within the grains with a few situated along the grain boundaries. These examinations proved an intragranular dispersion of TiC particles and it is evident that a strong interfacial bonding exists with matrix (Fig. 9a).

Dislocation formation can be attributed to two possible causes: (i) during FSVP processing, the matrix alloy undergoes extensive plastic deformation[29,30], and (ii) strain mismatch between TiC particles and the AZ31 alloy[29,30]. The frictional heat generated during processing did not completely eliminate dislocations. Dislocation-

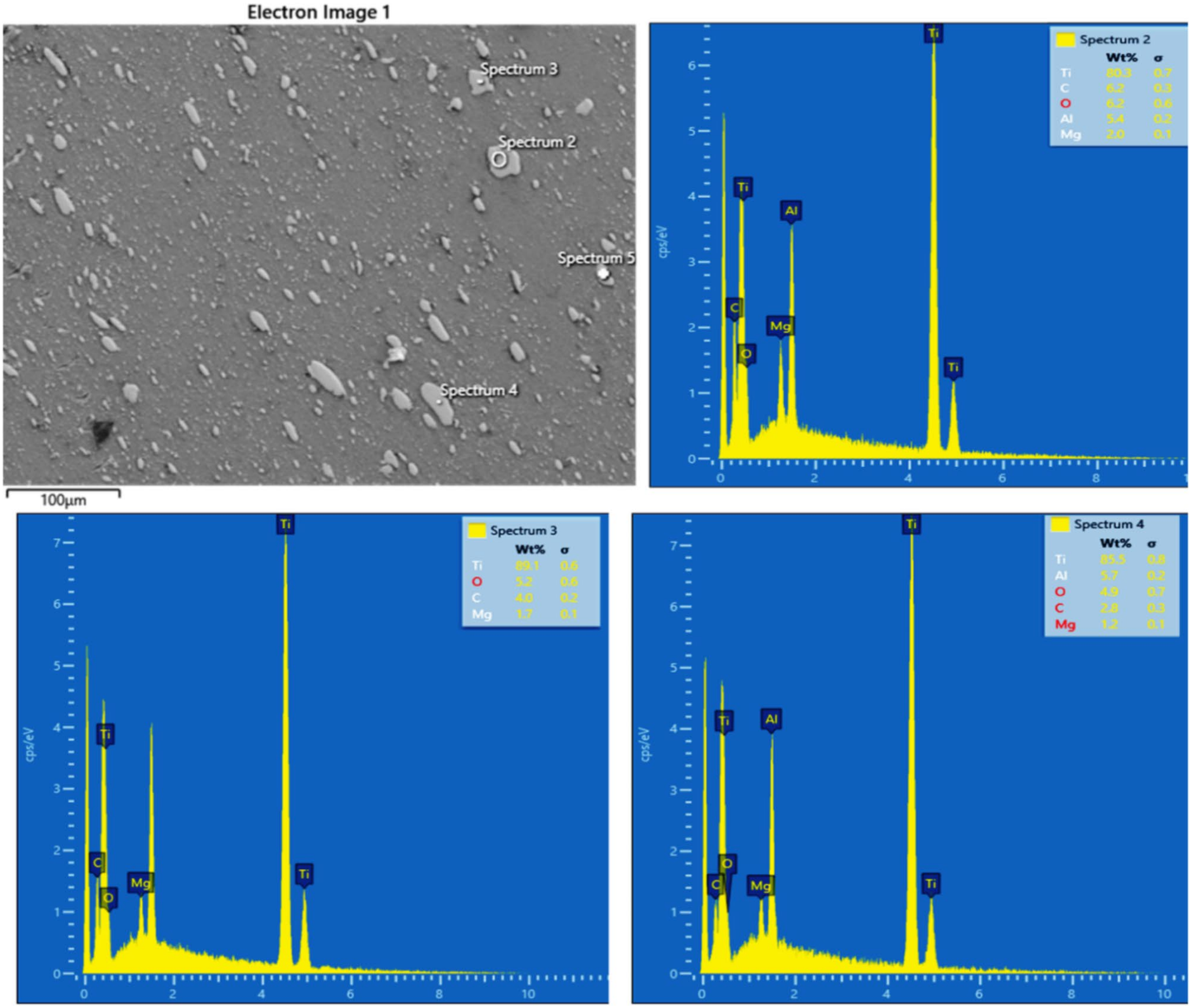

Fig. 6. SEM/EDS results at various regions of AZ31/15 vol% TiC FSVP surface composites.

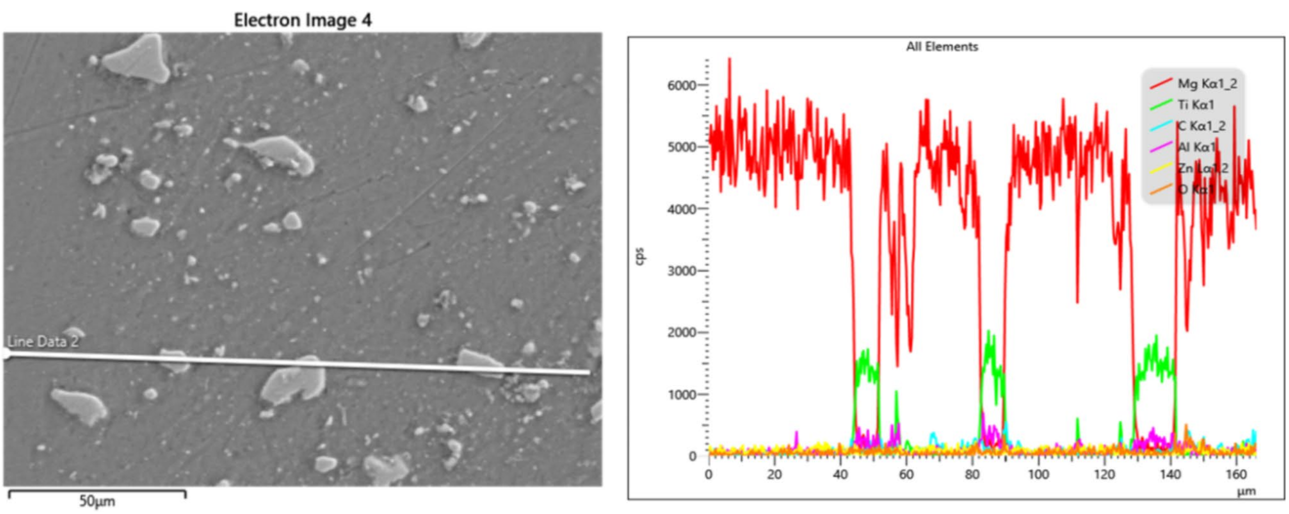

Fig. 7. Elemental distribution within AZ31/15 vol% TiC FSVP surface composites.

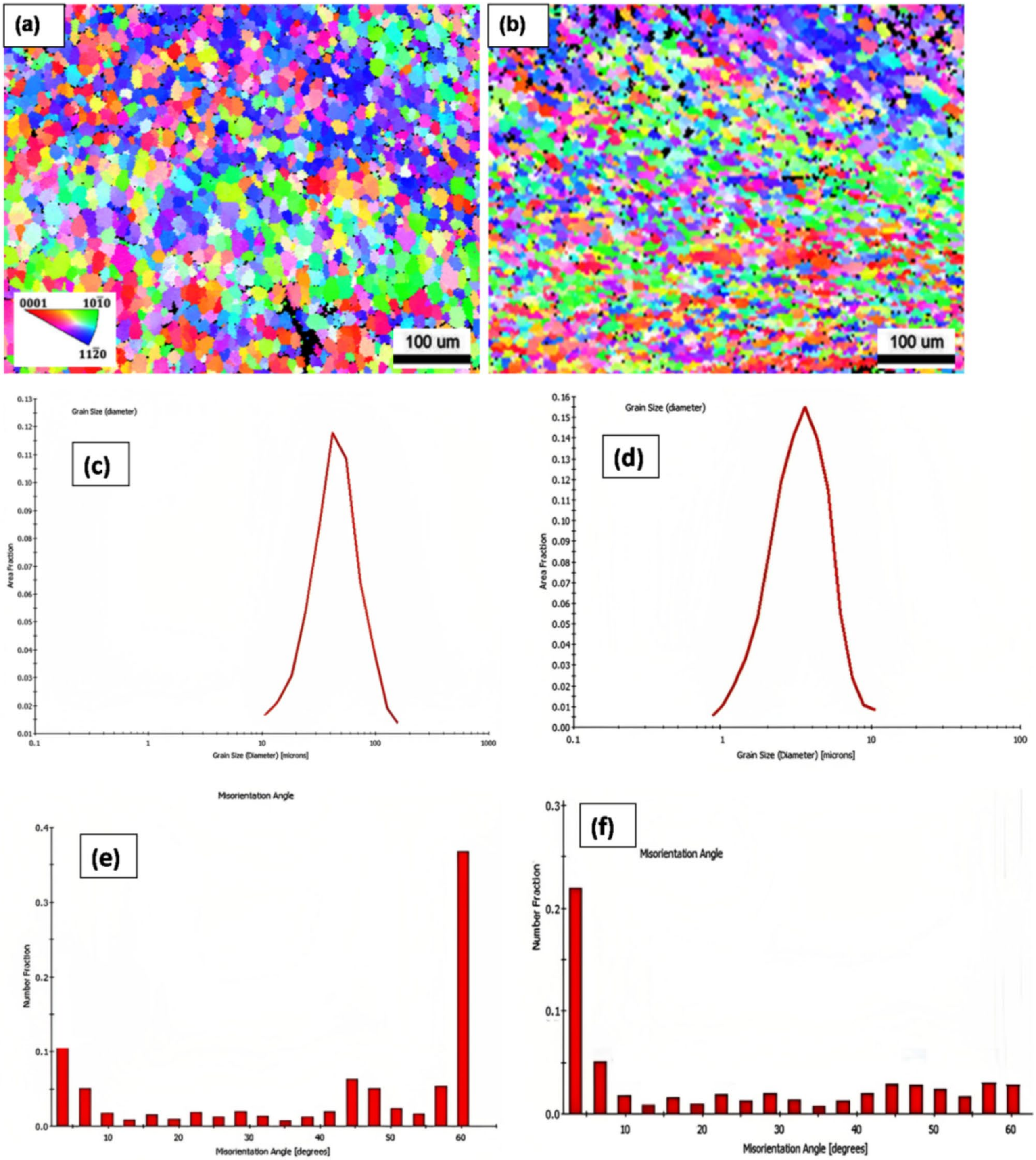

Fig. 8. EBSD (IPF + grain boundary) maps ofAZ31/ 15 vol% TiC composites produced via (**a**) FSP, (**b**) FSVP, (**c**) Grain size of the FSP sample, (**d**) Grain size of the FSVP sample, Misorientation distribution (**e**) FSP sample and (**f**) FSVP sample.

filled strain fields are known to contribute to the composite's strength. Particles of TiC experienced fracture during processing because of significant plastic deformation during FSVP. In addition to the pinning effect of smaller-sized broken particles, dynamic recrystallization resulted in a remarkable refinement of grains in the composite. Plastic deformation and the resulting strain mismatch led to the observation of dense dislocations in the matrix[31–33].

The variation in microhardness distribution across the transverse direction of AZ31 alloys subjected to FSP and FSVP is illustrated in Fig. 10a. It is evident that the inclusion of TiC particles and the application of

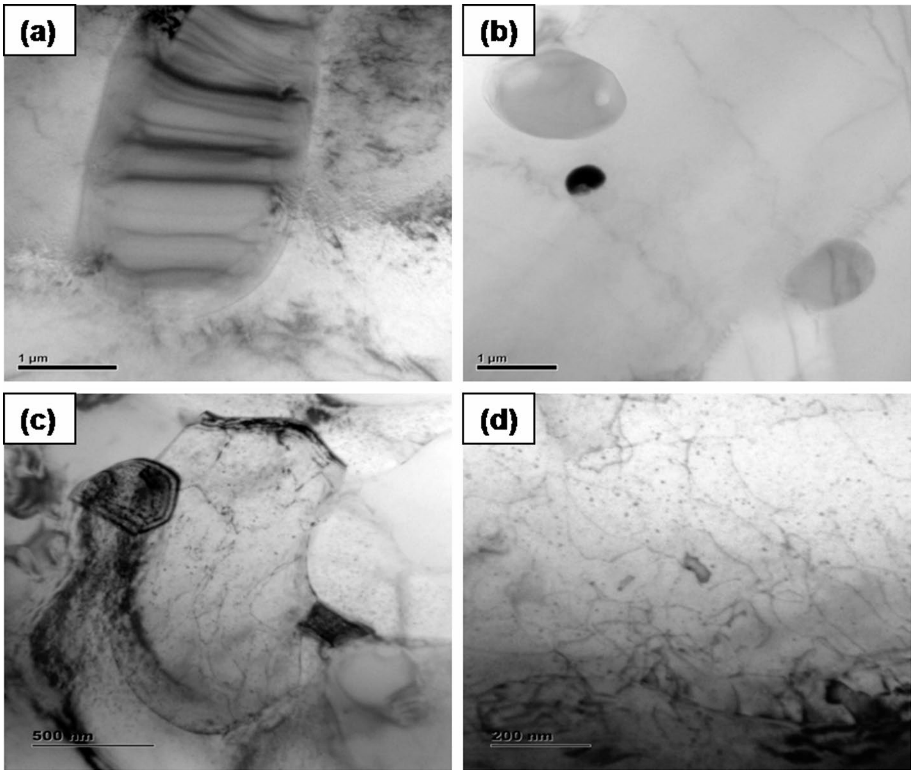

Fig. 9. TEM micrograph of AZ31/15vol% TiC FSVP surface composites showing; (**a**) AZ31/TiC particle interface, (**b**) TiC particle, (**c**) fine grains in AZ31 matrix and (**d**) dislocation density.

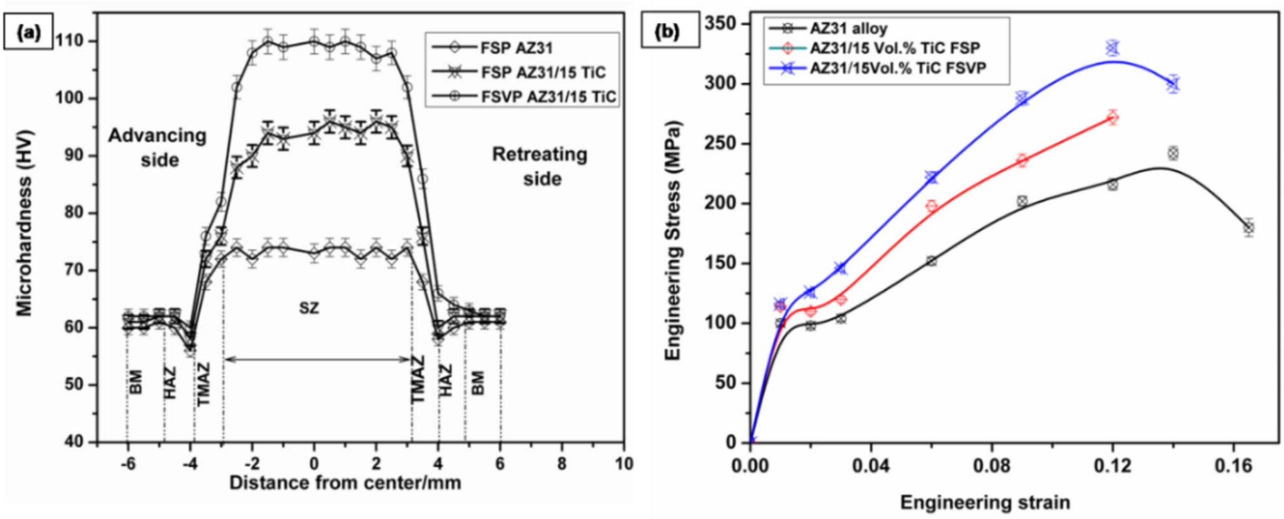

Fig. 10. (**a**) Hardness and (**b**) stress-strain plots of AZ31/15 vol. %TiC MMCs.

FSVP significantly improved the hardness of the AZ31 alloy. Considering the average microhardness value of 72 ± 2 HV for friction stir processed AZ31 alloy, the AZ31/15 vol% TiC surface composites fabricated via FSP demonstrated 94 ± 2 HV, while the same composition developed through FSVP showcased 114 ± 2 HV, marking an increase of 30% and 55%, respectively.

The tensile properties of AZ31/15 vol% TiC MMCs are depicted in Fig. 10b. The reinforcement of TiC particles into the AZ31 alloy to create these composites resulted in a significant increase in tensile strength. The ultimate tensile strength (UTS) was found to be 222 ± 6 MPa for 0 vol% TiC, 272 ± 6 MPa for 15 vol% TiC FSP, and 330 ± 7 MPa for 15 vol% TiC FSVP. This improvement in UTS can be attributed to the microstructural modifications caused by the incorporation of TiC particles and ultrasonic vibration. An increase in straining of the metal surface material due to vibration is associated with the reduction in grain size and improvement in mechanical characteristics. An increase in straining leads to a corresponding rise in dislocation density. Associated with dynamic recrystallization, it results in increased formation of high-angle grain boundaries[1,29,30]. The strengthening mechanisms at play in these composites are discussed below.

The disparity in coefficients of thermal expansion between the AZ31 matrix and the TiC particles generates dislocation density, and TiC becomes a hindrance to the free movement of dislocations. This obstruction contributes to a reinforcement process referred to as particle strengthening or dispersion strengthening. It enhances the material's ability to withstand deformation by increasing the energy needed to displace dislocations beyond the particles. As previously discussed, the TiC particles exhibit excellent bonding with the AZ31 alloy matrix without the development of pores or other compounds. This exceptional interfacial bonding allows for the efficient transfer of tensile loads to the TiC particles. The homogeneous distribution of TiC in the AZ31 matrix can activate the Orowan mechanism during tensile loading. Furthermore, the significant grain refinement in the TiC-added composite compared to the AZ31 alloy will enhance tensile strength in accordance with the Hall–Petch equation. Figure 10b clearly demonstrates a considerable degree of ductility retained in the composite after the tensile test. This increase in ductility can be attributed to the factors explained below.

Based on the rule of mixtures, AZ31 dispersed with TiC reinforcement should be stronger than pure AZ31, and from the study, it is observed that the addition of TiC enhanced the mechanical strength of the matrix metal and acts as a main source of strengthening. The uniform distribution of TiC particles within the matrix achieved through the FSP process is advantageous for Orowan strengthening. It retards the progression of dislocations and changes their direction of motion multiple times. Microstructures revealed strong bonding among TiC particles and the AZ31 matrix, facilitating effective transfer of tensile loads to the particles. The presence of dislocation-filled strain fields hindered the free movement of dislocations, thereby contributing to strength enhancement. The excellent grain refinement attained by FSVP, as per the Hall–Petch relationship, provides additional strengthening[34,35].

These factors interact with each other to strengthen the composite. Importantly, the presence of TiC particles does not significantly reduce ductility. This is due to the deformable nature of TiC particles under tensile load and their efficient heat conduction. This prevents excessive work hardening of the AZ31 alloy during the tensile test, which allows sufficient plastic flow of the AZ31 alloy. The presence of fine dimples on the tensile fracture surface is a result of grain structure refinement in the FSVP-based composite. The tensile fracture surfaces reveal that FSVP composites failed in a more ductile manner.

The tensile fracture surfaces of AZ31/15 vol% TiC composites synthesized via FSP and FSVP are depicted in Fig. 11a and b, respectively. The morphology observed in these images confirms that all specimens experienced plastic deformation before reaching the failure point. The development and coalescence of micro-voids were identified as the primary contributors to the ductile failure in all specimens. The AZ31/15 vol% TiC FSVP composites displayed smaller dimples, indicating more refined grain structure, while larger dimples were associated with the AZ31/15 vol% TiC FSP composites. The formation of fine dimples may be due to the significant grain refinement in the FSVP samples. The distribution of TiC particles on the fracture surface is evident from Fig. 11, indicating effective transfer of tensile loads due to proper interfacial bonding. These analyses of the fracture surfaces strongly suggest that the interfacial bonding was exceptionally effective.

Conclusions

In this study, a 6 mm thick AZ31 magnesium alloy dispersed with TiC reinforcing particles was fabricated using FSP and FSVP methods. The study aimed to compare the microstructure, hardness, and tensile properties of AZ31/15 vol% TiC surface composites produced via both FSP and FSVP. The key findings and conclusions of the study are summarized below —.

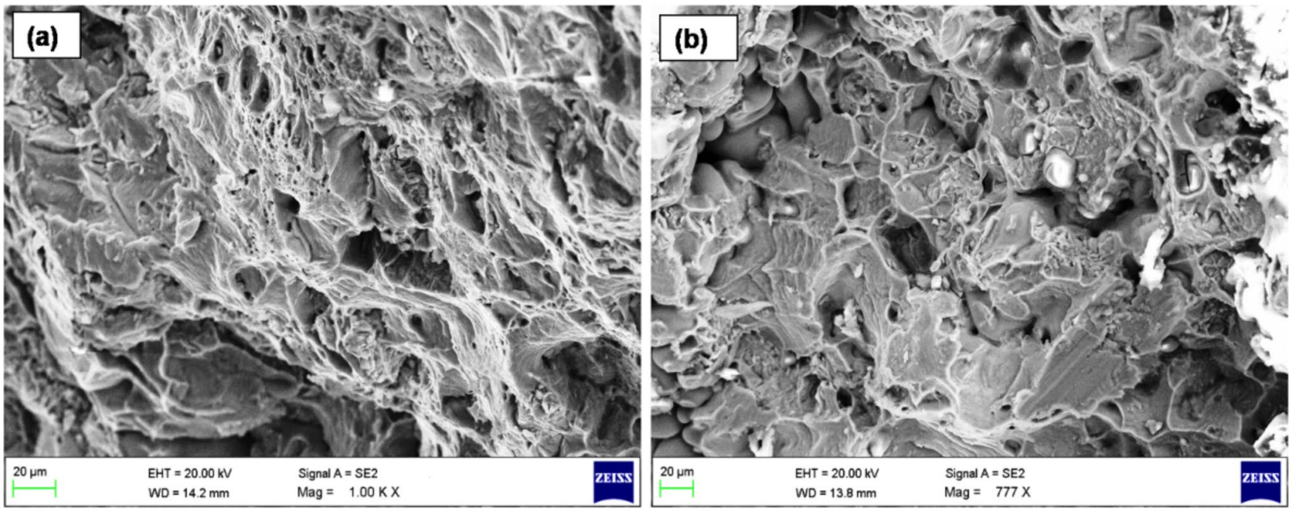

Fig. 11. Tensile fracture surface of AZ31/15 vol. %TiC composites (**a**) FSP and (**b**) FSVP.

1. The application of vibration during FSP effectively eliminated flow-related defects such as voids and tunneling. The use of vibration resulted in uniform dispersion of the TiC particles in the AZ31 matrix due to improved material flow and fluidity achieved by FSVP.
2. Processing the AZ31 alloy with 15 vol% TiC via FSP reduced the grain size from 60 to 28 µm. Using FSVP, the grain size in the AZ31/15 vol% TiC composite was further decreased to 8–10 µm.
3. Compared to the AZ31/15 vol% TiC FSP composite, composites produced via FSVP showed improvements in hardness and UTS of about 55% and 21%, respectively.
4. The retained ductility in Friction Stir Vibration Processed samples was related to the presence of fine grain structures, which led to the formation of well-developed dimples, thereby preserving the ductility of the samples.

Data availability
The data presented in this study are available through email upon request to the corresponding author.

Received: 23 April 2024; Accepted: 25 October 2024
Published online: 04 November 2024

References
1. Zhang, M. et al. Achieving high mechanical and wear properties in the AZ31/($CeO_2 + ZrO_2$) p surface composite using friction stir processing: Application of vibration. *Vacuum*. 218112654. https://doi.org/10.1016/j.vacuum.2023.112654 (2023).
2. Kumar, T. S., Thankachan, T. & Shalini, S. Microstructure, hardness and wear behaviour of ZrC particle reinforced AZ31 surface composites synthesized via friction stir processing. *Sci. Rep.* **13**, 20089. https://doi.org/10.1038/s41598-023-47381-5 (2023).
3. Kumar, T. S. et al. Development and characterization of AZ91/AlN magnesium matrix composites via friction stir processing. *AIP Adv.* **14**, 065301. https://doi.org/10.1063/5.0202057 (2024).
4. Zhu, C. et al. Proliferation and osteogenic differentiation of rat BMSCs on a novel Ti/SiC metal matrix nanocomposite modified by friction stir processing. *Sci. Rep.* **6**, 38875. https://doi.org/10.1038/srep38875 (2016).
5. Balakrishnan, M., Dinaharan, I., Palanivel, R. & Sivaprakasam, R. Synthesize of AZ31/TiC magnesium matrix composites using friction stir processing. *J. Magnes. Alloys* **3**(1), 76–78. https://doi.org/10.1016/j.jma.2014.12.007 (2015).
6. Navazani, M. & Dehghani, K. Investigation of microstructure and hardness of Mg/TiC surface composite fabricated by Friction Stir Processing (FSP). *Procedia Mater. Sci.* **11**, 509–514. https://doi.org/10.1016/j.mspro.2015.11.082 (2015).
7. Tian, C., Dai, X., Shi, L. & Wu, C. Enhancing the mechanical properties in the weld nugget zone of friction stir welded 2195 Al–Li alloy joint via superimposing ultrasonic vibration. *Vacuum*. **206**, 111540 (2022).
8. Liang, J. et al. Fabrication and mechanical properties of CNTs/Mg composites prepared by combining friction stir processing and ultrasonic assisted extrusion. *J. Alloys Compd.* **728**, 282–288 (2017).
9. Singla, S., Sagar, P. & Handa, A. Magnesium-based nanocomposites synthesized using friction stir processing: An experimental study. *Mater. Manuf. Process.* 1–18. https://doi.org/10.1080/10426914.2023.2195909 (2023).
10. Inácio, P. L. et al. Functionalized material production via multi-stack Upward Friction Stir Processing (UFSP). *Mater. Manuf. Process.* **37**, 11–24. https://doi.org/10.1080/10426914.2021.1942909 (2022).
11. Dehghani, K. & Mazinani, M. Forming nanocrystalline surface layers in copper using friction stir processing. *Mater. Manuf. Process.* **26**, 922–925. https://doi.org/10.1080/10426914.2011.564253 (2011).
12. Liu, T. et al. Achievement of high-quality joints and regulation of intermetallic compounds in ultrasonic vibration enhanced friction stir lap welding of Aluminum/Steel. *J. Mater. Res. Technol.* **25**, 5096–5109 (2023).
13. Lv, X. Q., Wu, C. S. & Padhy, G. K. Diminishing intermetallic compound layer in ultrasonic vibration enhanced friction stir welding of aluminum alloy to magnesium alloy. *Mater. Lett.* **203**, 81–84 (2017).
14. Swathi, I. B., Raju, L. S. & Rao, K. V. Optimization of ultrasonic vibration assisted friction stir process to improve mechanical properties of AA7075-nano B_4C surface composite. *Proc. Inst. Mech. Eng. Part C J. Mech. Eng. Sci.* **236**, 9012–9026. https://doi.org/10.1177/09544062221091471 (2022).
15. Liang, J. et al. Fabrication and mechanical properties of CNTs/Mg composites prepared by combining friction stir processing and ultrasonic assisted extrusion. *J. All Comp.* **728**, 282–288 (2017).
16. Bagheri, B. et al. The role of vibration and pass number on microstructure and mechanical properties of AZ91/SiC composite layer during friction stir processing. *Proc. I Mech. E Part. C J. MechEngSci*. https://doi.org/10.1177/09544062211024281 (2021).
17. Gao, S. & Wu, C. S. Padhy Material flow, microstructure and mechanical properties of friction stir welded AA 2024-T3 enhanced by ultrasonic vibrations. *J. Manuf. Process.* **30**, 385–395 (2017).
18. Kar, A., Suwas, S. & Kailas, S. V. Multi-length scale characterization of microstructure evolution and its consequence on mechanical properties in dissimilar friction stir welding of titanium to aluminum. *Metall. Mater. Trans. A*. **50**, 5153–5173. https://doi.org/10.1007/s11661-019-05409-4 (2019).
19. Edalati, K. et al. Formation metastable phases in magnesium–titanium system by high-pressure torsion their hydrogen storage performance. *Acta Mater.* **99**, 150–156 (2015).
20. Yu, H., Sun, Y., Hu, L., Wan, Z. & Zhou, H. Microstructure and properties of mechanically milled AZ61 powders dispersed with submicron/nanometer Ti particulates. *Mater. Char*. **127**, 272–278 (2017).
21. Yu, H., Sun, Y., Wan, Z., Zhou, H. & Hu, L. Nanocrystalline Ti/AZ61 magnesium matrix composite: Evolution of microstructure and mechanical property during annealing treatment. *J. Alloy Comp.* **741**, 231–239 (2018).
22. Sharma, V., Prakash, U. & Kumar, B. M. Surface composites by friction stir processing: A review. *J. Mater. Process. Technol.* **224**, 117–134 (2015).
23. Rathee, S., Maheshwari, S., Siddiquee, A. N. & Srivastava, M. A review of recent progress in solid state fabrication of composites and functionally graded systems via friction stir processing. *Crit. Rev. Solid State Mater. Sci.* **43**, 334–366 (2018).
24. Luo, J., Liu, S., Paidar, M., Vignesh, R. V. & Mehrez, S. Enhanced mechanical and tribological properties of AA6061/CeO_2 composite fabricated by friction stir processing. *Mater. Lett.* 318132210. https://doi.org/10.1016/j.matlet.2022.132210 (2022).
25. Paidar, M. et al. Development and characterization of dissimilar joint between AA2024-T3 and AA6061-T6 by modified friction stir clinching process. *Vacuum*. **176**, 109298. https://doi.org/10.1016/j.vacuum.2020.109298 (2020).
26. Krishna, S. A., Radhika, N., Saleh, B. & Manivannan, S. Microstructural mechanical and corrosion properties of SS304/HEA surface layer produced by Friction Stir Processing. *J. Alloys Compd.* **953**, 170153. https://doi.org/10.1016/j.jallcom.2023.170153 (2023).
27. Satish Kumar, T., Shalini, S. & Thankachan, T. Friction stir processing-based surface modification of AZ31 magnesium alloy. *Mater. Manuf. Process.* **38**, 1426–1435. https://doi.org/10.1080/10426914.2023.2165670 (2023).
28. Ding, Z. et al. Effects of friction stir processing on the phase transformation and microstructure of TiO_2-compounded Ti–6Al–4V alloy. *Metal Mater. Trans. A*. **47**, 5675–5679. https://doi.org/10.1007/s11661-016-3809-8 (2016).

29. Abbasi, M., Givi, M. & Bagheri, B. Application of vibration to enhance efficiency of friction stir processing. *Trans. Nonferrous Met. Soc. China* **29**, 1393–1400 (2019). https://doi.org/10.1016/S1003-6326(19)65046-6
30. Barati, M., Abbasi, M. & Abedini, M. the effects of friction stir processing and friction stir vibration processing on mechanical, wear and corrosion characteristics of Al6061/SiO_2 surface composite. *J. Manuf. Process.* **45**, 491–497. https://doi.org/10.1016/j.jmapro.2019.07.034 (2019).
31. Dinaharan, I., Zhang, S., Chen, G. & Shi, Q. Assessment of Ti–6Al–4V particles as a reinforcement for AZ31 magnesium alloy-based composites to boost ductility incorporated through friction stir processing. *J. Magnesium Alloys*. **10**(4), 979–992 (2022).
32. Maoliang, H., Shi, S. W. Q., Xu, Z. J. H. & Wang, Y. Dynamic recrystallization behaviour and mechanical properties of bimodal scale Al_2O_3 reinforced AZ31 composites by solid state synthesis. *J. Magnesium Alloys*. **8**(3), 841–848. https://doi.org/10.1016/j.jma.2020.02.012 (2020).
33. Li, F., Liu, Y. & Li, X. B. Dynamic recrystallization behaviour of AZ31 magnesium alloy processed by alternate forward extrusion. *Front. Mater. Sci.* **11**, 296–305. https://doi.org/10.1007/s11706-017-0387-7 (2017).
34. Cui, Y. W., Wang, L. & Zhang, L. C. Towards load-bearing biomedical titanium-based alloys: From essential requirements to future developments. *Prog. Mater. Sci.* **144**, 101277 (2024).
35. Liqiang Wang, Y. et al. Tensile and super elastic behaviors of Ti–35Nb–2Ta–3Zr with gradient structure. *Mater. Des.* (194), 108961. https://doi.org/10.1016/j.matdes.2020.108961 (2020).

Acknowledgements

This article was co-funded by the European Union under the REFRESH – Research Excellence For REgion Sustainability and High-tech Industries project number CZ.10.03.01/00/22_003/0000048 via the Operational Programme Just Transition and has been done in connection with project Students Grant Competition SP2024/087 „Specific Research of Sustainable Manufacturing Technologies“ financed by the Ministry of Education, Youth and Sports and Faculty of Mechanical Engineering VŠB-TUO.

Author contributions

Conceptualization: T.Satish Kumar, Titus Thankachan, Robert Čep, Kanak Kalita; Formal analysis: T. Satish Kumar, Titus Thankachan, Robert Čep, Kanak Kalita; Investigation: T. Satish Kumar, Titus Thankachan, Robert Čep, Kanak Kalita; Methodology: T. Satish Kumar, Titus Thankachan, Robert Čep, Kanak Kalita; Writing – original draft: T. Satish Kumar, Titus Thankachan, Robert Čep, Kanak Kalita; Writing – review & editing: T. Satish Kumar, Titus Thankachan, Robert Čep, Kanak Kalita; All authors have read and agreed to the published version of the manuscript.

Declarations

Competing interests

The authors declare no competing interests.

Additional information

Correspondence and requests for materials should be addressed to T.S.K. or K.K.

Reprints and permissions information is available at www.nature.com/reprints.

Publisher's note Springer Nature remains neutral with regard to jurisdictional claims in published maps and institutional affiliations.